ORGANOMETALLICS

ARTICLE

pubs.acs.org/Organometallics

Organometallic Pyridylnaphthalimide Complexes as Protein Kinase Inhibitors

Sebastian Blanck,[†] Thomas Cruchter,[†] Adina Vultur,[‡] Radostan Riedel,[†] Klaus Harms,[†] Meenhard Herlyn,[‡] and Eric Meggers*[,†]

[†]Fachbereich Chemie, Philipps-Universität Marburg, Hans-Meerwein-Strasse, 35043 Marburg, Germany

[‡]The Wistar Institute, 3601 Spruce Street, Philadelphia, Pennsylvania 19104, United States

Supporting Information

ABSTRACT: A new metal-containing scaffold for the design of protein kinase inhibitors is introduced. The key feature is a 3-(2-pyridyl)-1,8-naphthalimide "pharmacophore chelate ligand", which is designed to form two hydrogen bonds with the hinge region of the ATP-binding site and is at the same time capable of serving as a stable bidentate ligand through C−H activation at the 4-position of the electron-deficient naphthalene moiety. This C−H activation leads to a reduced demand for coordinating heteroatoms and thus sets the basis for a very efficient three-step synthesis starting from 1,8-naphthalic anhydride. The versatility of this ligand is demonstrated with the discovery of a ruthenium complex that functions as a nanomolar inhibitor for myosin light-chain kinase (MYLK or MLCK).

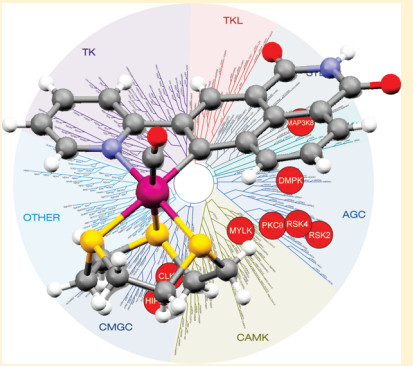

INTRODUCTION

The last two decades have witnessed a steadily growing interest for organometallic compounds in medicinal chemistry and chemical biology.[1] The unique properties of metal complexes such as structural diversity, adjustable ligand exchange kinetics, fine-tuned redox activities, photoreactivity, the availability of radioisotopes, and distinct spectroscopic signatures make them highly versatile scaffolds for the modulation, sensing, and imaging of biological processes.[2]

Several years ago we established a research program exploring substitutionally inert metal-containing compounds as structural scaffolds for the design of enzyme inhibitors, and we demonstrated that ruthenium(II),[3] platinum(II),[4] osmium(II),[5] and iridium(III)[6] complexes, for example, can serve as highly potent and selective inhibitors of protein kinases and lipid kinases.[7] We believe that especially octahedral coordination modes offer new opportunities to design globular and well-defined molecular shapes that can fill protein pockets such as enzyme active sites in unique ways.[8]

Our previous design was entirely based on the staurosporine-inspired metallo-pyridocarbazole scaffold shown in Figure 1, in which the maleimide moiety forms two key hydrogen bonds with the hinge region of the ATP-binding site, the pyridocarbazole heterocycle occupies the hydrophobic adenine binding cleft, and the remaining globular space-demanding octahedral or half-sandwich coordination sphere undergoes interactions in the region of the ribose-triphosphate binding site.[9] In this design strategy, the pyridocarbazole heterocycle—called "pharmacophore chelate ligand"—is rationally designed to interact with the hinge region of the ATP-binding site of protein kinases, whereas the remaining coordination sphere can then be established through combinatorial chemistry, structure−activity relationships, structure-based design, and combinations thereof. Although this approach turned out to be highly successful, we recently became interested in designing new pharmacophore chelate ligands for metal-containing protein kinase inhibitors for two reasons: First, the synthesis of the pyridocarbazole ligand is lengthy and includes one photochemical step, thus complicating derivatizations in the course of structure−activity relationships and inhibitor scale-up reactions for in vivo studies.[10] Second, we envisioned that placing the metal center at a different position within the ATP-binding site might allow us to discover metal-containing inhibitors with very different binding profiles. In this respect it is noteworthy that protein kinases are among the largest enzyme families with more than 500 putative protein kinase genes,[11] and we estimate that our previous pyridocarbazole metal complex scaffold is probably only suitable for a subset of them. Here we now introduce 3-(2-pyridyl)-1,8-naphthalimide (**1a**; Scheme 1) as such a novel pharmacophore ligand. It can be synthesized in just three steps from readily available 1,8-naphthalic anhydride and coordinates to ruthenium in a bidentate fashion by activating a C−H bond within the naphthalimide moiety, and as a proof of principle we report an organoruthenium complex which serves as a selective and nanomolar protein kinase inhibitor.

Received: May 3, 2011
Published: July 18, 2011

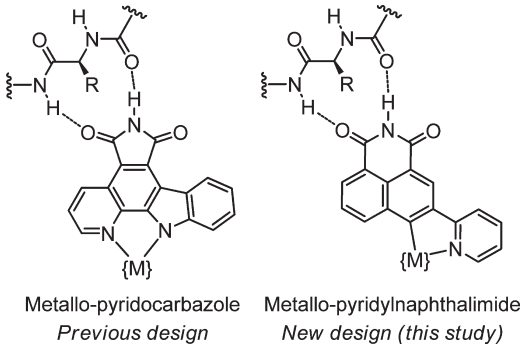

Figure 1. Previous and new design for metal complexes as protein kinase inhibitors. Shown are the intended interactions of the so-called "pharmacophore chelate ligand" with the hinge region of the ATP-binding site of protein kinases.

Scheme 1. Synthesis of 3-(2-Pyridyl)-1,8-naphthalimide (1a) and *N*-Benzyl-3-(2-pyridyl)-1,8-naphthalimide (1b)

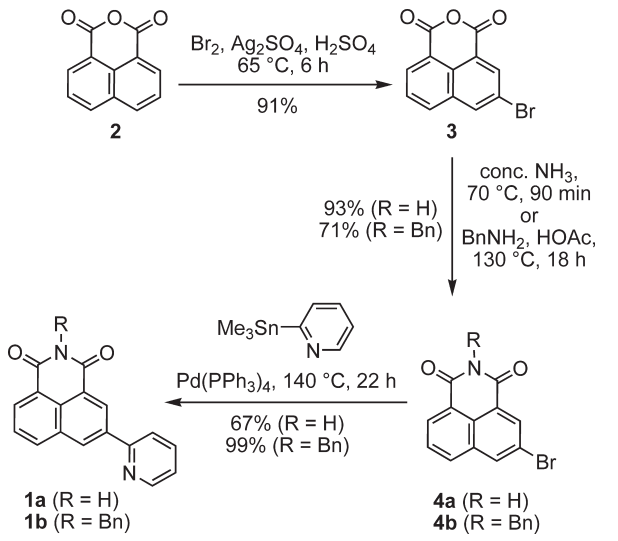

RESULTS AND DISCUSSION

Synthesis of the 3-(2-Pyridyl)-1,8-naphthalimide Ligand. The synthesis of the 3-(2-pyridyl)-1,8-naphthalimide ligand **1a** (R = H) and its benzylated derivative **1b** (R = Bn), which merely served as a crystallization handle, is outlined in Scheme 1. Accordingly, a bromination of 1,8-naphthalic anhydride **2** in concentrated sulfuric acid using silver(I) sulfate as catalyst afforded exclusively 3-bromo-1,8-naphthalic anhydride (**3**; 91%), which was further converted to the free imide **4a** (93%) or the benzyl-protected imide **4b** (71%) by treatment with concentrated ammonia or benzylamine, respectively. A subsequent Pd-mediated Stille cross coupling with 2-(trimethylstannyl)pyridine provided the final ligands **1a** (67%) and **1b** (99%) in three steps overall and total yields of 57% and 64%, respectively.

Synthesis of Half-Sandwich Compounds. To investigate the coordination properties of the new pyridylnaphthalimide ligands, we started with the synthesis of ruthenium half-sandwich complexes. For example, the reaction of the ligands **1a,b** with $[Ru(\eta^5\text{-}C_5H_5)(CO)(MeCN)_2]PF_6$[12] in the presence of Et_3N at 60 °C provided the complexes **5a** (51%) and **5b** (70%), which could be purified by standard silica gel flash chromatography (Scheme 2).

Scheme 2. Synthesis of Ruthenium Half-Sandwich Complexes 5a,b as Racemic Mixtures[a]

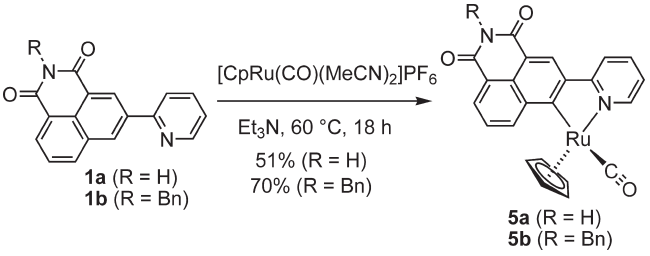

[a] Only one enantiomer is shown.

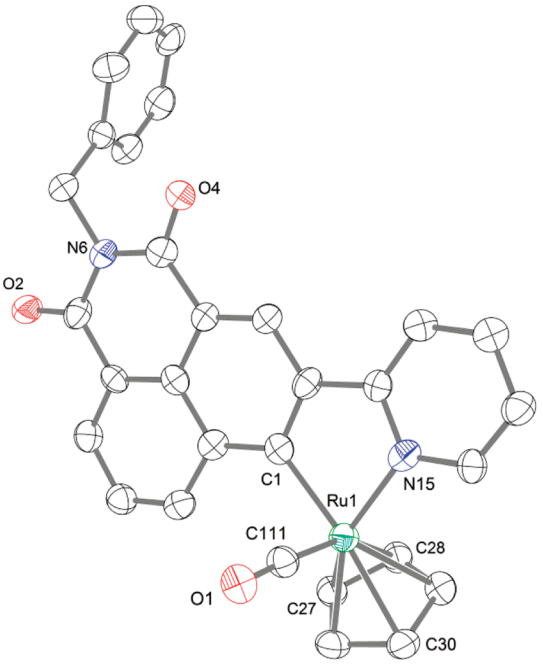

Figure 2. ORTEP drawing with 50% probability thermal ellipsoids, giving the crystal structure of half-sandwich complex **5b**. A disordered CH_2Cl_2 solvent molecule is omitted. Selected bond distances (Å) and angles (deg): Ru1−C1 = 2.073(8), Ru1−N15 = 2.094(9), Ru1−C27 = 2.230(10), Ru1−C30 = 2.274(7), Ru1−C111 = 1.838(12); C1−Ru−N15 = 78.8(4), C111−Ru1−C1 = 87.2(4), C111−Ru1−N15 = 97.0(4).

As anticipated, the C−H activation occurred solely at the 4-position of the naphthalimide moiety, while no C−H activation at the sterically more hindered 2-position was observed. A crystal structure of complex **5b** is displayed in Figure 2 and confirms the bidentate binding of the ruthenium to the pyridine nitrogen (Ru−N = 2.09 Å) and the C-4 atom of the naphthalene moiety (Ru−C = 2.07 Å). It is worth noting that the facile C−H activation and robustness of the formed Ru−C bond can be attributed to the highly electron deficient nature of the naphthalene moiety, being functionalized with electron-withdrawing pyridyl and maleimide substituents.[13]

Synthesis of Octahedral Complexes. In order to evaluate the synthesis of octahedral ruthenium complexes, ligand **1a** was reacted with $[Ru(MeCN)_3([9]aneS_3)](CF_3SO_3)_2$[14] ([9]aneS$_3$ = 1,4,7-trithiacylononane) and triethylamine in DMF at 60 °C to obtain the monoacetonitrile complex **6** in 77% yield (Scheme 3).

Scheme 3. Synthesis of the Octahedral 1,4,7-Trithiacyclononane Ruthenium Complexes 7−9 by Two Different Routes[a]

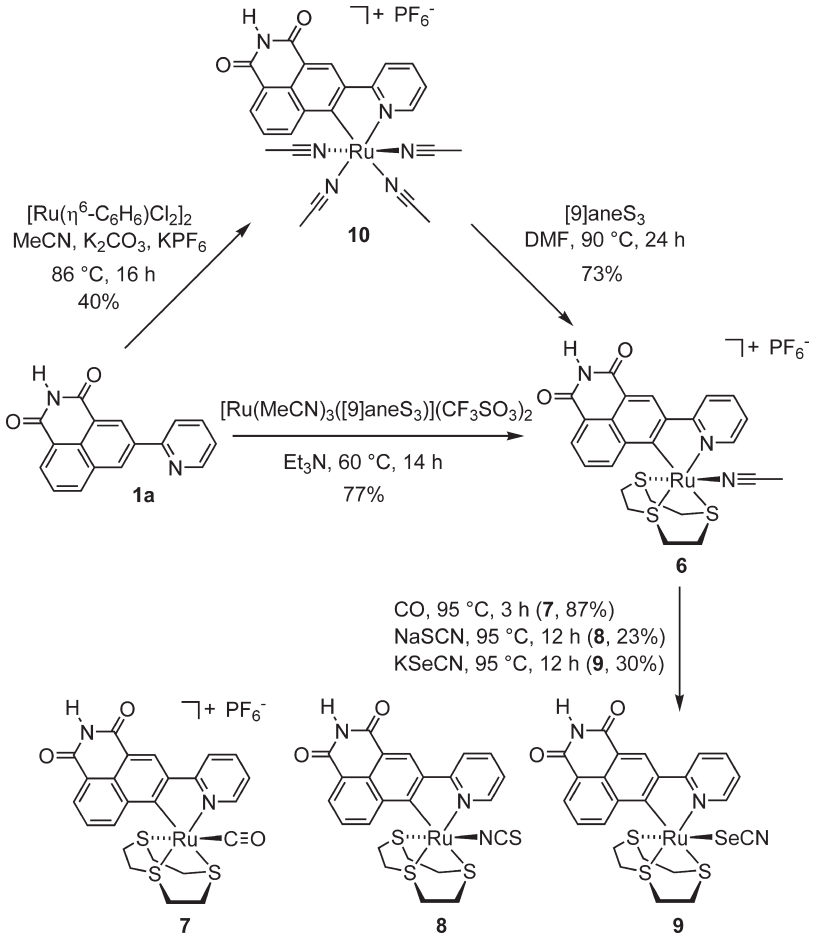

[a] Only one enantiomer of the formed racemic mixtures **6**−**9** is shown.

This complex offers a quick access to different octahedral complexes by exchanging the remaining semilabile acetonitrile with other monodentate ligands. For example, heating the acetonitrile complex **6** under an atmosphere of CO for 3 h provided the CO complex **7** in 87% yield. The synthesis of the thiocyanate complex **8** and the selenocyanate complex **9** were accomplished by reacting complex **6** with NaSCN (23% yield) and KSeCN (30% yield), respectively. All three complexes were purified by regular silica gel flash chromatography. As an example, complex **7** was tested for its stability under biologically relevant conditions and was found to be stable in aqueous solution under air in the presence of millimolar concentrations of 2-mercaptoethanol for several days without any sign of decomposition, as determined by ^{1}H NMR spectroscopy.

The crystal structure of complex **7** displayed in Figure 3 reveals that, in contrast to the half-sandwich complex **5b**, the pyridylnaphthalimide ligand in the octahedral complex is twisted, which is apparently due to a steric repulsion between the C−H group at the 5-position of the naphthalimide moiety and the sterically demanding 1,4,7-trithiacyclononane ligand. This steric repulsion also results in a significant distortion of the entire octahedral ruthenium coordination geometry. For example, the CO ligand is not oriented perpendicular to the plane of the naphthalimide moiety but instead is bent backward. Interestingly, the crystal structure furthermore demonstrates the desired ability of the imide moiety to form hydrogen bonds.

Synthesis of a Reactive "Precursor Complex". For future combinatorial chemistry it would be desirable to have access to a complex in which the ruthenium is coordinated to the pyridylnaphthalimide pharmacophore ligand in addition to labile monodentate coordinating ligands that can be replaced in a combinatorial fashion against other mono-, bi-, tri-, or even tetradentate ligands, thus providing rapid access to a diversity of novel structures just by straightforward ligand substitution chemistry.[15] In fact, the reaction of pyridylnaphthalimide **1a** with $[Ru(\eta^6\text{-}C_6H_6)Cl_2]_2$ in the presence of K_2CO_3 and KPF_6 in refluxing acetonitrile afforded in one step the tetraacetonitrile complex **10** in a yield of 40% (Scheme 3).[16] The crystal structure of complex **10** is shown in Figure 4. Despite the apparent lability of the four acetonitrile ligands, complex **10** is surprisingly robust and can be purified by regular silica gel flash chromatography. As expected, the acetonitrile ligands of **10** are prone to substitution at elevated temperature. For example, the reaction of **10** with 1,4,7-trithiacyclononane in DMF provided in a good yield of 73% the complex **6**, in which three acetonitrile ligands have been replaced by 1,4,7-trithiacyclononane.

Protein Kinase Inhibition. To quickly gain insight into the protein kinase inhibition properties of pyridylnaphthalimide metal complexes, we tested complex **7** as a representative member of this class of compounds for its protein kinase binding affinity profile against the majority of the human protein kinases encoded in the human genome (human kinome).[11] This was accomplished

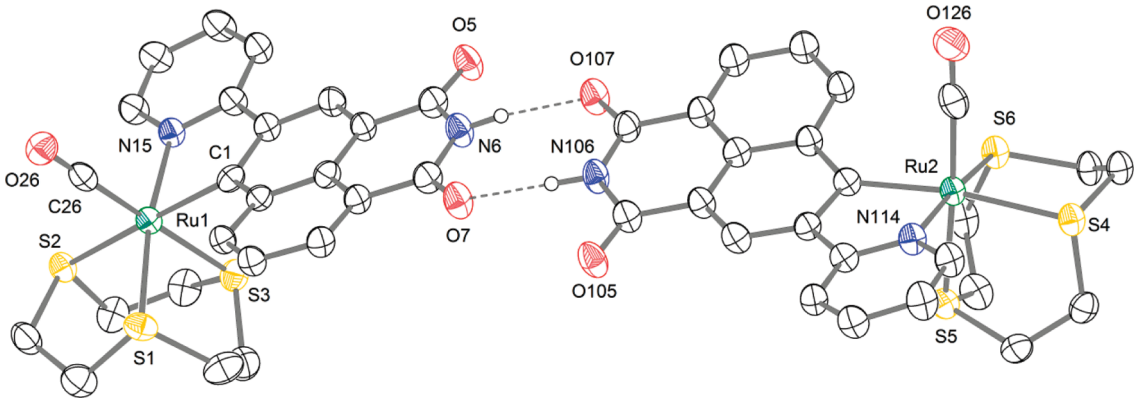

Figure 3. ORTEP drawing with 50% probability thermal ellipsoids, giving the crystal structure of the 1,4,7-trithiacyclononane complex **7**. Solvent molecules (MeCN and diethyl ether) and the hexafluorophosphate counterions are omitted for clarity. Selected bond distances (Å) and angles (deg): Ru1−C1 = 2.075(4), Ru1−N15 = 2.095(4), Ru1−C26 = 1.864(5), Ru1−S1 = 2.3419(11), Ru1−S2 = 2.4169(11), Ru1−S3 = 2.4077(12); C1−Ru1−N15 = 78.72(15), C1−Ru1−S3 = 87.53(12), C1−Ru1−C26 = 92.29(17), N15−Ru1−S3 = 84.01(10), N15−Ru1−C26 = 94.91(16).

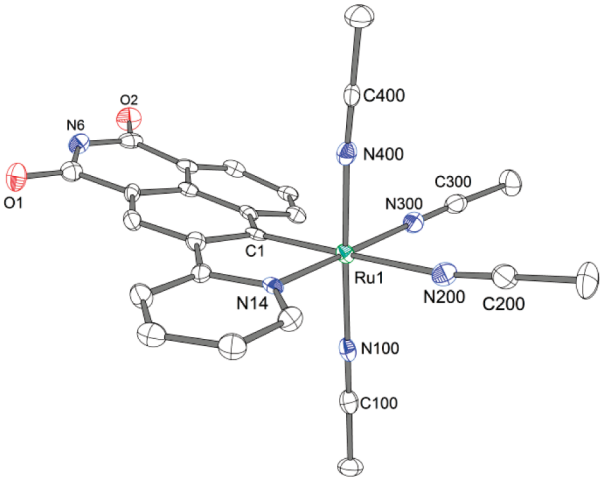

Figure 4. ORTEP drawing with 50% probability thermal ellipsoids, giving the crystal structure of the tetraacetonitrile precursor complex **10**. Selected bond distances (Å) and angles (deg): Ru1−C1 = 2.041(4), Ru1−N14 = 2.043(4), Ru1−N100 = 2.018(4), Ru1−N200 = 2.165(4), Ru1−N300 = 2.049(4), Ru1−N400 = 2.018(4); C1−Ru1−N14 = 80.35(15), C1−Ru1−N100 = 92.06(15), C1−Ru1−N200 = 175.11(16), C1−Ru1−N300 = 102.31(15), C1−Ru1−N400 = 90.49(15), C100−N100−Ru1 = 179.4(4), C200−N200−Ru1 = 169.0(4), C300−N300−Ru1 = 168.4(3), C400−N400−Ru1 = 174.5(3).

by using an active-site-directed competition binding assay with 442 different protein kinases (KINOME*scan*, DiscoveRx) which provides primary data (%ctrl = percent of control: 0% = highest affinity, 100% = no affinity) that correlate with binding constants (K_d).[17,18] Interestingly, out of the 442 enzymes tested, 8 protein kinases, namely CLK2, DMPK, HIPK2, MAP3K8, MYLK, PKCθ, RSK2, and RSK4, were identified as the main hits with %ctrl values below 0.1%. The human kinase dendrogram shown in Figure 5 reveals that these eight kinases are distributed among four protein kinase families. We selected myosin light-chain kinase (MYLK or MLCK) for further studies because MYLK plays a very important role in smooth muscle contraction.[19] Upon stimulation by agonists, the intracellular concentration of Ca^{2+} of smooth muscle is elevated, causing Ca^{2+} to bind to calmodulin. The complex of Ca^{2+} and calmodulin then activates MYLK. We determined complex **7** to be a nanomolar inhibitor of

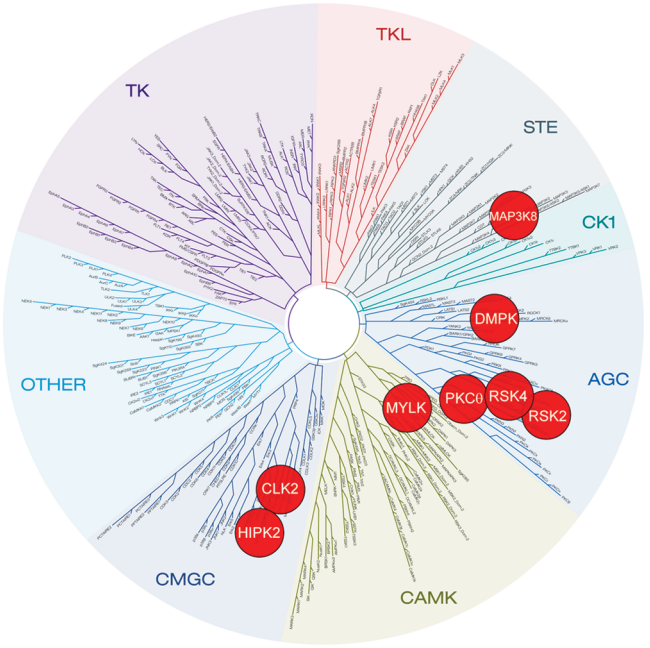

Figure 5. Protein kinase selectivity of complex **7** as determined by an active-site-directed affinity screening (KINOME*scan*, DiscoveRx) against 442 human protein kinases: representation of the main hits (<0.1% of control; 0% = highest affinity, 100% = no affinity) within the human kinase dendrogram, which displays the protein kinase families and the evolutionary relationships between the individual kinases. See the Supporting Information for additional data.

MYLK with an IC_{50} value (concentration of inhibitor at which the enzyme activity is reduced to 50%) of 75 ± 20 nM (100 μM ATP), which according to the Cheng−Prusoff equation (K_m(ATP) = 50 μM) would reflect an inhibition constant (K_d) of approximately 25 nM.[20,21] Surprisingly, the pyridyl-naphthalimide ligand **1a** itself does not show any sign of MYLK inhibition even at a concentration of 1 mM. Thus, the Ru(1,4,7-trithiacyclononane)(CO) fragment increases the binding affinity by more than 4 orders of magnitude. To evaluate if complex **7** binds as designed to the hinge region of the ATP-binding site, we synthesized a derivative of **7** in which the imide hydrogen is replaced by a methyl group (**7Me**). As shown in Figure 6, this

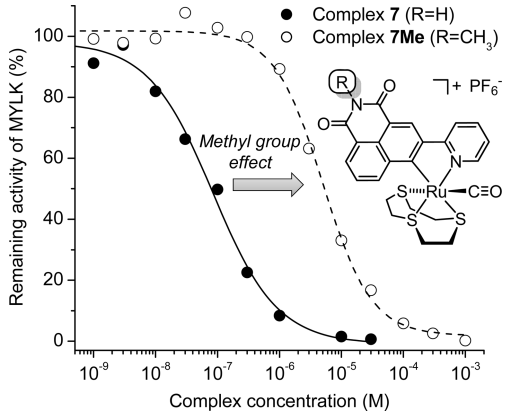

Figure 6. IC_{50} curves of complex **7** and the methylated control complex **7Me** against MYLK at an ATP concentration of 100 μM. The pyridylnaphthalimide ligand **1a** does not show any inhibition of MYLK even at a concentration of 1 mM.

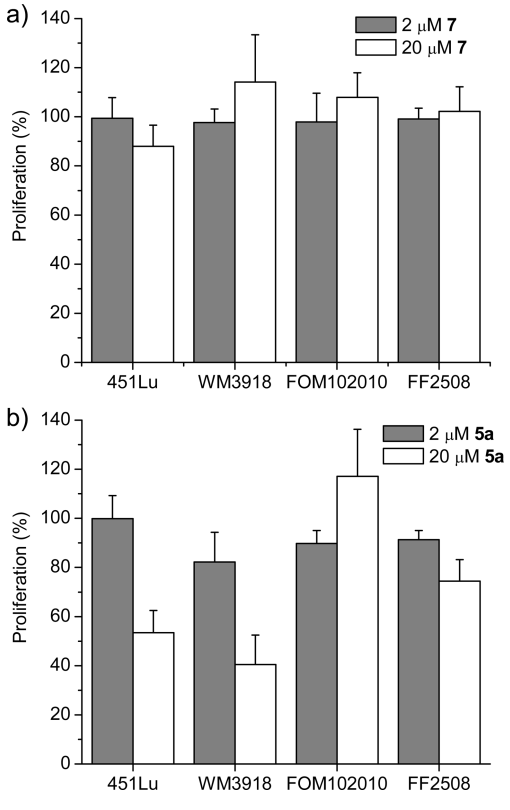

Figure 7. Effects of the pyridylnapthalimide complexes **7** and **5a** on the proliferation of human-derived cells. Cellular proliferations of melanoma cell lines (451Lu and WM3918), human melanocytes (FOM102010), and human fibroblasts (FF2508) were assessed with the MTS assay. Data show the mean value of three independent experiments, including the standard deviations. The proliferation is given as the percent of DMSO control experiments.

methylation dramatically reduces the activity by almost 2 orders of magnitude (IC_{50} = 5.2 ± 1.0 μM), consistent with the expectation that the imide hydrogen forms a hydrogen bond with a carbonyl oxygen of the hinge region, as indicated in Figure 1. It is also worth noting that neither the half-sandwich complex **5a** (IC_{50} = 83 ± 36 μM) nor the thiocyanate **8** (IC_{50} of 3.5 ± 0.9 μM) or selenocyanate **9** (IC_{50} = 4.2 ± 1.3 μM) display any significant affinity for MYLK, indicating that it is the bent position of the coordinated CO that is crucial for MYLK binding, most likely through a specific interaction with a region of the flexible glycine-rich loop.

Acitivities in Human Cells. Finally, because of the recent clinical success of kinase inhibitors for the treatment of metastatic melanoma,[22,23] we investigated complexes **5a** and **7** as representative members of the new class of metallo-naphthalimides in an in vitro MTS proliferation assay[24] with two human-derived melanoma cell lines (451Lu and WM3918), as well as human melanocytes (FOM102010) and human fibroblast cells (FF2508) as controls (Figure 7). Unfortunately, even at a concentration as high as 20 μM, complex **7** did not show any significant effects on the melanoma or normal human cell lines (Figure 7a). It can be assumed that this is due to the cationic nature of complex **7**, which may prevent an efficient cellular uptake. In fact, in contrast to complex **7**, the neutral complex **5a** inhibited the proliferation of the melanoma cell lines 451Lu and WM3918 in a dose-dependent fashion to 53% and 40% at 20 μM, respectively, while fibroblasts were only slightly affected and melanocytes not at all (Figure 7b). Thus, due to this promising therapeutic window, complex **5a** and derivatives thereof should be further evaluated for their antimelanoma activities.

CONCLUSIONS

In summary, we have introduced 3-(2-pyridyl)-1,8-napthalimide as a novel pharmacophore chelate ligand for metal-based protein kinase inhibitors and demonstrated its versatility by presenting a ruthenium complex as a nanomolar inhibitor of myosin light-chain kinase. 3-(2-Pyridyl)-1,8-naphthalimide is designed to interact with the hinge region of the ATP-binding site by forming two hydrogen bonds with the imide moiety. A key feature is its capability of serving as a stable bidentate ligand through C−H activation at the 4-position of the electron-deficient naphthalene moiety, which simplifies the structure by reducing the number of required heteroatoms for transition-metal binding.

EXPERIMENTAL SECTION

General Methods. All reactions were carried out using oven-dried glassware and conducted under a positive pressure of nitrogen unless otherwise specified. 1,8-Naphthalic anhydride, silver(I) sulfate, and other chemicals were used as received from standard suppliers unless otherwise specified. 3-Bromo-1,8-naphthalic anhydride,[25] 2-(trimethylstannyl)pyridine,[26] tetrakis(triphenylphosphine)palladium(0),[27] $[Ru(\eta^5\text{-}C_5H_5)(CO)(MeCN)_2]PF_6$,[12] $[Ru(MeCN)_3([9]aneS_3)](CF_3SO_3)_2$,[14] and $[RuCl_2(\eta^6\text{-}C_6H_6)]_2$[28] were prepared according to literature procedures. All solvents were distilled prior to use. Acetonitrile and DMF were dried by common methods and freshly distilled prior to use. NMR spectra were recorded on an Avance 300 (300 MHz), DRX-400 (400 MHz), Avance 500 (500 MHz), or DRX-500 (500 MHz) spectrometer. Infrared spectra were recorded on a Bruker Alpha FTIR instrument . High-resolution mass spectra were obtained with a Finnigan LTQ-FT instrument using either APCI or ESI. Complex **7Me** was synthesized analogously to **7** (see the Supporting Information).

3-Bromo-1,8-naphthalimide (4a). 3-Bromo-1,8-naphthalic anhydride (**3**; 5.07 g, 18.3 mmol) was added to 255 mL of concentrated ammonia (28%) and heated to 70 °C for 90 min. The solution was cooled to ambient temperature, and the resulting precipitate was filtered off, washed with ethanol twice, and dried under vacuum to provide 3-bromo-1,8-naphthalimide (**4a**) as an off-white solid (4.71 g, 93%). ^{1}H

NMR (300 MHz, DMSO-d_6): δ (ppm) 11.82 (br s, 1H), 8.70 (d, J = 2.1 Hz, 1H), 8.34−8.43 (m, 3H), 7.87 (t, J = 7.8 Hz, 1H). ^{13}C NMR (75 MHz, DMSO-d_6): δ (ppm) 163.7, 162.9, 135.7, 133.3, 132.9, 131.7, 130.2, 128.2, 127.2, 124.5, 122.7, 119.9. IR (film): ν (cm^{-1}) 3180, 3067, 2827, 1693, 1617, 1589, 1408, 1326, 1262, 883, 821, 783, 745, 726, 515, 477, 429. HRMS: m/z calcd for $C_{12}H_7BrNO_2$ $(M + H)^+$ 277.9634, found 277.9624.

3-(2-Pyridyl)-1,8-naphthalimide (1a). 3-Bromo-1,8-naphthalimide (**3**; 0.95 g, 3.44 mmol) and 2-(trimethylstannyl)pyridine (0.84 g, 3.47 mmol) were dissolved in 15 mL of *m*-xylene, and the reaction mixture was purged with nitrogen for 15 min. Tetrakis(triphenylphosphine)-palladium(0) (197 mg, 0.17 mmol) was added and the mixture was heated to reflux for 22 h. After the mixture was cooled to ambient temperature, the solvent was removed and the crude product adsorbed onto silica gel, and subjected to silica gel chromatography with CH_2Cl_2/MeOH (75/1). The combined product eluents were dried in vacuo, and 3-(2-pyridyl)-1,8-naphtalimide (**1a**) was obtained as a pale yellow solid (0.63 g, 67%). ^{1}H NMR (300 MHz, DMSO-d_6): δ (ppm) 11.77 (s, 1H), 9.11−9.13 (m, 2H), 8.76−8.78 (m, 1H), 8.52 (dd, J = 8.1, 0.9 Hz, 1H), 8.42 (dd, J = 7.2, 0.9 Hz, 1H), 8.23 (d, J = 8.1 Hz, 1H), 7.99 (td, J = 7.8, 1.8 Hz, 1H), 7.87 (dd, J = 8.1, 7.4 Hz, 1H), 7.47 (ddd, J = 7.5, 4.8, 0.9 Hz, 1H). ^{13}C NMR (75 MHz, DMSO-d_6): δ (ppm) 164.0, 154.2, 149.8, 137.6, 137.0, 134.9, 132.0, 131.4, 130.2, 128.7, 127.9, 127.5, 123.5, 123.1, 122.5, 120.8. IR (film): ν (cm^{-1}) 3174, 3064, 2846, 1672, 1595, 1586, 1414, 1381, 1360, 1337, 1259, 1203, 843, 833, 780, 748, 737, 513, 500, 475, 439, 401. HRMS: m/z calcd for $C_{17}H_{10}N_2O_2Na$ $(M + Na)^+$ 297.0634, found 297.0633.

***N*-Benzyl-3-bromo-1,8-naphthalimide (4b).** 3-Bromo-1,8-naphthalic anhydride (**3**; 3.00 g, 10.8 mmol) was suspended in 75 mL of glacial acetic acid, benzylamine (1.78 mL, 16.2 mmol) was added, and the reaction mixture was heated to reflux for 18 h. The reaction mixture was carefully poured into ice-cold water, and the resulting beige precipitate was filtered off and washed with water. The crude product was dissolved in CH_2Cl_2, adsorbed onto silica gel, and subjected to silica gel chromatography with CH_2Cl_2/hexane (3/2). The combined product eluents were dried in vacuo to provide *N*-benzyl-3-bromo-1,8-naphtalimide (**4b**) as an off-white solid (2.82 g, 71%). ^{1}H NMR (300 MHz, $CDCl_3$): δ (ppm) 8.66 (d, J = 2.1 Hz, 1H), 8.59 (dd, J = 7.8, 1.2 Hz, 1H), 8.34 (d, J = 2.1 Hz, 1H), 8.01 (dd, J = 8.4, 0.9 Hz, 1H), 7.76 (dd, J = 8.4, 7.5 Hz, 1H), 7.53−7.56 (m, 2H), 7.24−7.34 (m, 3H), 5.37 (s, 2H). ^{13}C NMR (75 MHz, $CDCl_3$): δ (ppm) 163.6, 163.0, 137.0, 135.5, 134.1, 132.82, 132.75, 131.5, 129.1, 128.5, 128.0, 127.6, 126.5, 124.1, 122.8, 121.1, 43.7. IR (film): ν (cm^{-1}) 3065, 3033, 1702, 1662, 1621, 1587, 1432, 1407, 1358, 1322, 1232, 1177, 1154, 1074, 827, 732, 701. HRMS: m/z calcd for $C_{19}H_{13}BrNO_2$ $(M + H)^+$ 368.0106, found 368.0102.

***N*-Benzyl-3-(2-pyridyl)-1,8-naphthalimide (1b).** *N*-Benzyl-3-bromo-1,8-naphthalimide (**4b**; 417 mg, 1.14 mmol) and 2-(trimethylstannyl)pyridine (250 mg, 1.04 mmol) were dissolved in 25 mL of *m*-xylene, and the reaction mixture was purged with nitrogen for 15 min. Tetrakis(triphenylphosphine)palladium(0) (120 mg, 0.10 mmol) was added and the mixture heated to reflux for 22 h. After cooling to ambient temperature the solvent was removed, the crude product adsorbed onto silica gel, and subjected to silica gel chromatography with CH_2Cl_2/MeOH (75/1 to 35/1). The combined product eluents were dried in vacuo, and *N*-benzyl-3-(2-pyridyl)-1,8-naphthalimide (**1b**) was obtained as a pale yellow solid (381 mg, 99%). ^{1}H NMR (300 MHz, $CDCl_3$): δ (ppm) 9.17 (d, J = 1.8 Hz, 1H), 8.95 (d, J = 1.8 Hz, 1H), 8.76−8.78 (m, 1H), 8.59 (dd, J = 7.2, 1.2 Hz, 1H), 8.28 (dd, J = 8.1, 0.9 Hz, 1H), 7.96 (dt, J = 8.1, 0.9 Hz, 1H), 7.85 (td, J = 7.5, 1.8 Hz, 1H), 7.75 (dd, J = 8.1, 7.5 Hz, 1H), 7.56−7.59 (m, 2H), 7.24−7.36 (m, 4H), 5.41 (s, 2H). ^{13}C NMR (75 MHz, $CDCl_3$): δ (ppm) 164.2, 164.1, 155.2, 150.1, 138.0, 137.3, 137.2, 134.8, 132.1, 131.9, 131.7, 129.8, 129.0, 128.4, 128.2, 127.5, 127.4, 123.1, 122.6, 120.8, 43.6. IR (film): ν (cm^{-1}) 3062, 1701, 1662, 1626, 1591, 1476, 1420, 1331, 1200, 1180, 782, 736, 701. HRMS: m/z calcd for $C_{24}H_{17}N_2O_2$ $(M + H)^+$ 365.1285, found 365.1281.

Complex 5a. 3-(2-Pyridyl)-1,8-naphthalimide (**4a**; 30 mg, 108 μmol), and $[Ru(\eta^5\text{-}C_5H_5)(CO)(MeCN)_2]PF_6$ (71 mg, 165 μmol) were dissolved in 5 mL of DMF and the reaction mixture was purged with nitrogen for 10 min. Following the addition of triethylamine (35 μL, 249 μmol), the mixture was heated to 60 °C for 18 h. The reaction mixture was cooled to ambient temperature, diluted with 50 mL of CH_2Cl_2, and washed with saturated NH_4Cl solution. The aqueous phase was washed with 2 × 25 mL of CH_2Cl_2, the combined organic phases were dried using $MgSO_4$, and the crude product was subjected to silica gel chromatography with CH_2Cl_2/MeOH (40/1). The combined product eluents were dried in vacuo, and the final complex **5a** was obtained as a yellow solid (27 mg, 51%). ^{1}H NMR (300 MHz, DMSO-d_6): δ (ppm) 11.56 (s, 1H), 9.11 (d, J = 5.7 Hz, 1H), 8.76 (s, 1H), 8.53 (d, J = 8.4 Hz, 1H), 8.44−8.47 (m, 2H), 8.01 (t, J = 7.5 Hz, 1H), 7.80 (t, J = 7.8 Hz, 1H), 7.23 (t, J = 6.6 Hz, 1H), 5.29 (s, 5H). ^{13}C NMR (75 MHz, DMSO-d_6): δ (ppm) 201.0, 200.8, 165.9, 164.8, 164.1, 157.7, 144.7, 143.9, 142.8, 142.2, 137.9, 130.3, 125.7, 123.3, 122.7, 121.6, 120.4, 117.3, 85.1. IR (film): ν (cm^{-1}) 2922, 2851, 1934, 1670, 1577, 1557, 1471, 1381, 1318, 1257, 1244, 999, 965, 791, 777, 741. HRMS: m/z calcd for $C_{23}H_{15}N_2O_3Ru$ $(M + H)^+$ 469.0121, found 469.0123.

Complex 5b. *N*-Benzyl-3-(2-pyridyl)-1,8-naphthalimide (**4b**; 16 mg, 44 μmol) and $[Ru(\eta^6\text{-}C_5H_5)(CO)(MeCN)_2]PF_6$ (28 mg, 66 μmol) were dissolved in 4 mL of DMF, and the reaction mixture was purged with nitrogen for 10 min. Following the addition of triethylamine (7.3 μL, 53 μmol), the mixture was heated to 60 °C for 18 h. The solvent was removed and the crude product subjected to silica gel chromatography with CH_2Cl_2. The combined product eluents were dried in vacuo, and the complex **5b** was obtained as an orange solid (18 mg, 70%). ^{1}H NMR (400 MHz, $CDCl_3$): δ (ppm) 8.92 (d, J = 5.2 Hz, 1H), 8.83 (s, 1H), 8.65 (dd, J = 7.6, 1.2 Hz, 1H), 8.48 (dd, J = 8.4, 1.2 Hz, 1H), 8.09 (d, J = 8.0 Hz, 1H), 7.81 (td, J = 8.4, 1.6 Hz, 1H), 7.70 (t, J = 8.0 Hz, 1H), 7.55−7.57 (m, 2H), 7.28−7.32 (m, 2H), 7.20−7.24 (m, 1H), 7.00 (td, J = 6.6, 1.2 Hz, 1H), 5.44 (s, 2H), 5.08 (s, 5H). ^{13}C NMR (100 MHz, $CDCl_3$): δ (ppm) 202.6, 199.8, 167.2, 165.4, 164.4, 157.1, 144.1, 142.8, 142.5, 137.8, 137.0, 131.9, 128.7, 128.4, 127.2, 125.5, 124.6, 122.9, 120.6, 119.9, 117.3, 84.5, 43.4. IR (film): ν (cm^{-1}) 2925, 2854, 1930, 1690, 1649, 1581, 1561, 1474, 1390, 1319, 1229, 1180, 779, 731, 701. HRMS: m/z calcd for $C_{30}H_{21}N_2O_3Ru$ $(M + H)^+$ 559.0598, found 559.0608.

Complex 6. *Method a.* 3-(2-Pyridyl)-1,8-naphthalimide (**1a**; 70 mg, 255 μmol) and $[Ru(MeCN)_3([9]aneS_3)](CF_3SO_3)_2$ (269 mg, 383 μmol) were dissolved in 5 mL of DMF, triethylamine (92 μL, 663 μmol) was added, and the reaction mixture was heated to 60 °C for 14 h. The solution was cooled to ambient temperature, the solvent was removed, and the crude product was subjected to silica gel chromatography, first with acetonitrile, followed by acetonitrile/water/saturated KNO_3 solution (50/3/1). The combined product eluents were dried in vacuo, the residue was dissolved in a minimal amount of acetonitrile/water, and NH_4PF_6 was added. The solution was centrifuged, and the resulting orange filter cake was washed three times with water and dried in vacuo to provide the monoacetonitrile **6** complex as an orange solid (145 mg, 77%).

Method b. Tetraacetonitrile complex **10** (15 mg, 22 μmol) was dissolved in 3 mL of DMF, 1,4,7-trithiacyclonane was added, and the mixture was heated to 90 °C for 24 h. The solution was cooled to ambient temperature, the solvent was removed, and the crude product was subjected to silica gel chromatography, first with acetonitrile followed by acetonitrile/water/saturated KNO_3 solution (50/3/1). The combined product eluents were dried in vacuo, the residue was dissolved in a minimal amount of acetonitrile/water, and NH_4PF_6 was added. The solution was centrifuged, and the resulting orange filter cake was washed three times with water and dried in vacuo to provide monoacetonitrile complex **6** as an orange solid (12 mg, 73%). ^{1}H NMR

Table 1. Crystallographic Data for Ruthenium Complexes 5b, 7, and 10[a]

	5b·1.3CH_2Cl_2	**7**·Et_2O·CH_3CN	**10**
formula	$C_{30}H_{20}N_2O_3Ru$, 0.65CH_2Cl_2	$[C_{24}H_{21}N_2O_3RuS_2]^+$, PF_6^-, Et_2O, CH_3CN	$[C_{25}H_{21}N_6O_2Ru]^+$, PF_6^-
fw	612.88	883.88	683.52
a(Å)	23.7464(13)	12.6950(4)	8.3493(6)
b (Å)	7.0753(5)	14.1048(4)	11.6436(8)
c (Å)	29.415(2)	21.4127(7)	14.5174(8)
α (deg)		102.734(2)	102.461(5)
β (deg)		95.437(3)	101.109(5)
γ (deg)		99.004(3)	101.134(5)
V (Å^3)	4942.2(6)	3660.4(2)	1311.06(15)
Z	8	4	2
space group	*Pbca*	$P\bar{1}$	$P\bar{1}$
d_{calcd} (Mg/m^3)	1.647	1.604	1.731
μ (mm^{-1})	0.814	0.716	0.739
θ range (deg)	1.38−25	4.65−25	4.71−25
no. of indep rflns	3082	12 812	4476
no. of params	381	960	391
wR2 (all data)[b]	0.121	0.136	0.059
R1 ($I > 2\sigma(I)$)[b]	0.053	0.051	0.040
CCDC no.[c]	812716	812717	812718

[a] Mo Kα radiation (λ = 0.71073 Å). [b] R1 = $\Sigma||F_o| - |F_c||/\Sigma|F_o|$; wR2 = $[\Sigma w(F_o^2 - F_c^2)^2/\Sigma w(F_o^2)^2]^{1/2}$. [c] Crystallographic data (excluding structure factors) have been deposited with the Cambridge Crystallographic Data Center. CIF files can be obtained from the CCDC free of charge via http://www.ccdc.cam.ac.uk/data_request/cif.

(300 MHz, CD_3CN): δ (ppm) 9.39 (s, 1H), 8.95 (d, J = 8.4 Hz, 1H), 8.86 (s, 1H), 8.77 (d, J = 5.7 Hz, 1H), 8.55 (d, J = 7.2 Hz, 1H), 8.37 (d, J = 6.9 Hz, 1H), 8.08 (t, J = 7.5 Hz, 1H), 7.85 (t, J = 7.8 Hz, 1H), 7.38 (t, J = 6.9 Hz, 1H), 3.15−3.31 (m, 2H), 2.76−3.00 (m, 6H), 2.08−2.46 (m, 7H). ^{13}C NMR (75 MHz, CD_3CN): δ (ppm) 194.4, 189.9, 165.4, 164.5, 163.9, 153.1, 144.9, 141.5, 139.4, 139.0, 130.8, 129.5, 126.7, 124.0, 123.7, 123.6, 121.7, 119.4, 37.0, 36.5, 34.5, 33.6, 31.8, 30.6. IR (film): ν (cm^{-1}) 2991, 1974, 1675, 1582, 1564, 1476, 1412, 1386, 1322, 1248, 837, 778, 748. HRMS: m/z calcd for $C_{25}H_{24}N_3O_2RuS_3$ $(M - PF_6)^+$ 596.0069, found 596.0078.

Complex 7. The monoacetonitrile complex **6** (15 mg, 20 μmol) was dissolved in 4 mL of DMF and purged with CO gas for 30 s. The solution was heated to 95 °C for 3 h. The solvent was removed and the crude product subjected to silica gel chromatography, first with acetonitrile followed by acetonitrile/water/saturated KNO_3 solution (50/3/1). The combined product eluents were dried in vacuo, the residue was dissolved in a minimal amount of acetonitrile/water, and NH_4PF_6 was added. The solution was centrifuged, and the resulting yellow filter cake was washed three times with water and dried in vacuo to provide monoacetonitrile complex **7** as a yellow solid (13 mg, 87%). ^{1}H NMR (400 MHz, CD_3CN): δ (ppm) 9.36 (s, 1H), 8.95 (dd, J = 8.4, 1.2 Hz, 1H), 8.86 (s, 1H), 8.77 (dt, J = 5.2, 0.8 Hz, 1H), 8.55 (dd, J = 7.2, 1.2 Hz, 1H), 8.37 (d, J = 8.0 Hz, 1H), 8.08 (td, J = 8.4, 0.8 Hz, 1H), 7.85 (dd, J = 8.4, 7.2 Hz, 1H), 7.38 (td, J = 5.6, 1.2 Hz, 1H), 3.17−3.30 (m, 2H), 2.86−3.00 (m, 4H), 2.77−2.85 (m, 2H), 2.28−2.46 (m, 3H), 2.19−2.25 (m, 1H). ^{13}C NMR (100 MHz, CD_3CN): δ (ppm) 194.4, 189.9, 165.4, 164.5, 163.9, 153.1, 144.9, 141.5, 139.4, 138.9, 130.8, 129.4, 126.7, 124.0, 123.7, 123.6, 121.7, 119.4, 37.0, 36.5, 34.5, 33.6, 31.8, 30.6. IR (film): ν (cm^{-1}) 3164, 3053, 2839, 1991, 1675, 1584, 1474, 1387, 1317, 1266, 834, 780, 745. HRMS: m/z calcd for $C_{24}H_{21}N_2O_3RuS_3$ $(M - PF_6)^+$ 582.9752, found 582.9752.

Complex 8. The monoacetonitrile complex **6** (16 mg, 22 μmol) was dissolved in 2 mL of DMF, NaSCN (3 mg, 32 μmol) in water (100 μL) was added, and the solution was heated to 95 °C for 12 h. The solvent was removed and the crude product subjected to silica gel chromatography with CH_2Cl_2/MeOH (gradient 20/1 to 10/1). The combined product eluents were dried in vacuo, and the thiocyanate complex **8** was obtained as a red solid (3 mg, 23%). The ruthenium coordination of the ambidente NCS ligand through nitrogen was verified by ^{15}N NMR and the crystal structure of a benzylated derivative (see the Supporting Information). ^{1}H NMR (300 MHz, DMSO-d_6): δ (ppm) 11.42 (s, 1H), 9.22 (dd, J = 8.4, 1.1 Hz, 1H), 8.96 (d, J = 4.8 Hz, 1H), 8.64 (s, 1H), 8.40 (dd, J = 7.2, 0.9 Hz, 1H), 8.31 (d, J = 8.1 Hz, 1H), 7.90 (dt, J = 8.4, 1.5 Hz, 1H), 7.74 (dd, J = 7.6, 6.6 Hz, 1H), 7.31−7.36 (m, 1H), 3.14−3.20 (m, 1H), 2.87−2.97 (m, 2H), 2.64−2.76 (m, 5H), 2.07−2.19 (m, 1H), 1.83−2.01 (m, 3H). ^{13}C NMR (125 MHz, DMSO-d_6): δ (ppm) 215.2, 165.6, 165.4, 164.6, 152.6, 145.2, 143.1, 140.4, 137.0, 130.3, 129.1, 125.2, 124.3, 123.4, 122.8, 122.3, 119.9, 115.3, 36.6, 35.5, 35.2, 31.5, 30.3, 29.9. IR (film): ν (cm^{-1}) 3159, 3002, 2920, 2854, 2096, 1673, 1574, 1379, 1312, 1248, 1016, 951, 841, 768, 739. HRMS: m/z calcd for $C_{24}H_{21}N_3O_2RuS_4Na$ $(M + Na)^+$ 635.9453, found 635.9467.

Complex 9. The monoacetonitrile complex **6** (16 mg, 22 μmol) was dissolved in 2 mL of DMF, KSeCN (5 mg, 32 μmol) in water (100 μL) was added, and the solution was heated to 95 °C for 12 h. The solvent was removed and the crude product subjected to silica gel chromatography with CH_2Cl_2/MeOH (gradient 20/1 to 10/1). The combined product eluents were dried in vacuo, and the selenocyanate complex **9** was obtained as a red solid (4 mg, 30%). The ruthenium coordination of the ambidente SeCN ligand through selenium was verified by the crystal structure of a benzylated derivative (see the Supporting Information). ^{1}H NMR (500 MHz, DMSO-d_6): δ (ppm) 11.39 (s, 1H), 9.22 (dd, J = 8.0, 1.0 Hz, 1H), 8.94−8.95 (m, 1H), 8.64 (s, 1H), 8.39 (dd, J = 7.0, 1.0 Hz, 1H), 8.29 (d, J = 8.5 Hz, 1H), 7.90 (ddd, J = 8.5, 7.5, 1.5 Hz, 1H), 7.73 (dd, J = 8.5, 7.0 Hz, 1H), 7.32 (ddd, J = 7.0, 5.5, 1.5 Hz, 1H), 3.15−3.19 (m, 1H), 2.90−2.98 (m, 2H), 2.64−2.77 (m, 4H), 2.50−2.54 (m, 1H), 2.06−2.13 (m, 1H), 1.87−1.99 (m, 3H). ^{13}C NMR (125 MHz, DMSO-d_6): δ (ppm) 165.6, 165.3, 164.4, 152.5, 145.4, 143.2, 140.7, 137.0, 136.9, 130.4, 129.4, 125.0, 123.5, 122.8, 122.3, 119.9, 115.3, 108.4, 36.5, 36.3, 35.3, 31.3, 31.1, 30.0. IR (film): ν (cm^{-1}) 3344, 3224,

3003, 2921, 2851, 2098, 1674, 1575, 1507, 1432, 1406, 1378, 1321, 1256, 1019, 827, 778. HRMS: m/z calcd for $C_{24}H_{21}N_3O_2RuS_3SeNa$ $(M + Na)^+$ 683.8904, found 683.8903.

Complex 10. 3-(2-Pyridyl)-1,8-naphthalimide (**1a**; 78 mg, 0.28 mmol), $[RuCl_2(\eta^6\text{-}C_6H_6)]_2$ (71 mg, 0.14 mmol), KPF_6 (199 mg, 1.08 mmol), and K_2CO_3 (110 mg, 0.80 mmol) were dissolved in acetonitrile and heated to reflux for 16 h. The solvent was removed and the crude product subjected to silica gel chromatography with CH_2Cl_2/MeOH (gradient 35/1 to 20/1). The combined product eluents were dried in vacuo, and the tetraacetonitrile complex **10** was obtained as a red solid (77 mg, 40%). ^{1}H NMR (300 MHz, CD_3CN): δ (ppm) 9.21 (br s, 1H), 9.14 (dd, J = 8.4, 1.2 Hz, 1H), 9.04−9.06 (m, 1H), 8.65 (s, 1H), 8.52 (dd, J = 7.2, 1.2 Hz, 1H), 8.15 (d, J = 8.4 Hz, 1H), 7.85−7.91 (m, 1H), 7.78 (dd, J = 8.4, 7.2 Hz, 1H), 7.28 (ddd, J = 7.2, 5.7 Hz, 1.2 Hz, 1H), 2.55 (s, 3H), 2.14 (s, 6H), 1.99 (s, 3H). ^{13}C NMR (125 MHz, CD_3CN): δ (ppm) 215.8, 167.2, 165.0, 164.1, 152.7, 145.8, 143.4, 140.6, 136.8, 130.3, 128.8, 126.2, 124.8, 123.4, 122.2, 121.7, 121.5, 118.9, 115.6, 2.8. IR (film): ν (cm^{-1}) 3363, 2924, 2851, 2271, 1681, 1578, 1561, 1473, 1316, 1242, 830, 776, 757, 557. HRMS: m/z calcd for $C_{23}H_{18}N_5O_2Ru$ $(M - CH_3CN - PF_6)^+$ 498.0505, found 498.0487.

Protein Kinase Assays. The protein kinase selectivity profile of complex **7** at an assay concentration of 10 μM was derived from an active-site-directed affinity screening against 442 human protein kinases (KINOME*scan*, DiscoveRx). See the Supporting Information for additional data. For the determination of IC_{50} values, various concentrations of the ruthenium complexes or the ligand **1a** were incubated at room temperature in 20 mM MOPS, 30 mM $Mg(OAc)_2$, 0.8 μg/μL BSA, 5% DMSO (**7**−**9**, **7Me**), or 10% DMSO (**5a** and **1a**) (resulting from the inhibitor stock solution) at pH 7.0 in the presence of $CaCl_2$ (500 μM), calmodulin (1 μM), substrate ZIPtide (62.5 μM), and human MYLK (purchased from Millipore as MLCK) (6.9 nM). After 30 min, the reaction was initiated by adding ATP to a final concentration of 100 μM and approximately 0.1 μCi/μL $^{[\gamma\text{-}33P]}$ATP. Reactions were performed with a total volume of 25 μL. After 45 min, the reaction was terminated by spotting 15 μL on a circular P81 phosphocellulose paper (2.1 cm diameter, Whatman), followed by washing three times with 0.75% phosphoric acid and once with acetone. The dried P81 papers were transferred to a scintillation vial, 5 mL of scintillation cocktail was added, the counts per minute (CPM) were measured with a Beckmann Coulter™ LS6500 Multi-Purpose Scintillation Counter, and the IC_{50} values were defined to be the concentration of inhibitor at which the counts per minute (CPM) were 50% of the control sample, corrected by the background CPM.

Cell Viability Assays. Human melanoma cell lines (451Lu, WM3918) were isolated as previously described[29] and were further cultured in Dulbecco's modified Eagle's medium supplemented with 5% fetal bovine serum. Normal human primary melanocytes (FOM102010) and fibroblasts (FF2508) were isolated from the human epidermis of neonatal foreskins and cultured as described.[30,31] Cells (5000/well) were seeded in 96-well plates and allowed to adhere overnight. The following day, complex **5a**, **7**, or DMSO vehicle control was added to the cells at different concentrations and the cells were incubated for another 96 h. Cells were then directly incubated with MTS substrate (CellTiter-96 Aqueous One Solution Cell Proliferation Assay, Promega).[24] The absorbance was measured at 490 nm as per the supplier's instructions, and the percent proliferation was normalized to the absorbance of DMSO-treated cells. For each cell line and treatment, the absorbance values of at least 4 wells were used to analyze the data.

Single-Crystal X-ray Diffraction Studies. The intensity data sets for all compounds were collected at 100 K using a STOE IPDS2 (**5b**) or IPDS-2T (**7**, **10**) system. The data were corrected for absorption effects using multiscanned reflections (**5b**)[32] or indexed faces (**7**, **10**),[33] respectively. The structures were solved using direct methods (SIR-92[34] for **10** and SIR2008[35] for **5b**, **7**) and refined using the full-matrix least-squares procedure implemented in SHELX-97.[36] Hydrogen atoms were included at calculated positions, N-bonded H atoms in **10** were located and refined isotropically. The crystal of **5b** was twinned. Only the reflections of one twin domain were used for refinement. In **5b** two positions of a disordered CH_2Cl_2 molecule were refined with a total occupation of 0.65 in the asymmetric unit. In **7** one hexafluorophosphate anion was disordered. High displacement factors indicate non esolved disorder of the solvent ether molecules. Crystallographic data for **5b**, **7**, and **10** are given in Table 1.

■ ASSOCIATED CONTENT

Supporting Information. Figures, text, and tables giving screening data of compound **7** against a panel of 442 protein kinases, stability test with **7**, investigation of the binding mode of the ambidente thiocyanate and selenocyanate ligands in complexes **8** and **9**, synthesis and analytical data of the complex **7Me**, and the complete references 17, 18, and 22, and CIF files giving crystallographic data for **5b**, **7**, and **10**. This material is available free of charge via the Internet at http://pubs.acs.org.

■ AUTHOR INFORMATION

Corresponding Author

*E-mail: meggers@chemie.uni-marburg.de.

■ ACKNOWLEDGMENT

We thank the US National Institutes of Health (Grant No. CA114046) for support of this research. S.B. acknowledges a stipend from the Fonds der Chemischen Industrie.

■ REFERENCES

(1) For organometallics in biological and medicinal chemistry, see: (a) Severin, K.; Bergs, R.; Beck, W. *Angew. Chem., Int. Ed.* **1998**, *37*, 1634–1654. (b) Jaouen, G., Ed. *J. Organomet. Chem.* **1999**, *589*, 1−126. (c) Metzler-Nolte, N. *Angew. Chem., Int. Ed.* **2001**, *40*, 1040–1043. (d) Fish, R. H.; Jaouen, G. *Organometallics* **2003**, *22*, 2166–2177. (e) Schatzschneider, U.; Metzler-Nolte, N. *Angew. Chem., Int. Ed.* **2006**, *45*, 1504–1507. (f) Alberto, R. *J. Organomet. Chem.* **2007**, *692*, 1179–1186. (g) Hartinger, C. G.; Dyson, P. J. *Chem. Soc. Rev.* **2009**, *38*, 391–401. (h) Fish, R. H. *Aust. J. Chem.* **2010**, *63*, 1505–1513. (i) Hillard, E. A.; Jaouen, G. *Organometallics* **2011**, *30*, 20–27. (j) Gasser, G.; Ott, I.; Metzler-Nolte, N. *J. Med. Chem.* **2011**, *54*, 3–25.

(2) Haas, K. L.; Franz, K. J. *Chem. Rev.* **2009**, *109*, 4921–4960.

(3) (a) Debreczeni, J. É.; Bullock, A. N.; Atilla, G. E.; Williams, D. S.; Bregman, H.; Knapp, S.; Meggers, E. *Angew. Chem., Int. Ed.* **2006**, *45*, 1580–1585. (b) Maksimoska, J.; Feng, L.; Harms, K.; Yi, C.; Kissil, J.; Marmorstein, R.; Meggers, E. *J. Am. Chem. Soc.* **2008**, *130*, 15764–15765.

(4) Williams, D. S.; Carroll, P. J.; Meggers, E. *Inorg. Chem.* **2007**, *46*, 2944–2946.

(5) Maksimoska, J.; Williams, D. S.; Atilla-Gokcumen, G. E.; Smalley, K. S. M.; Carroll, P. J.; Webster, R. D.; Filippakopoulos, P.; Knapp, S.; Herlyn, M.; Meggers, E. *Chem. Eur. J.* **2008**, *14*, 4816–4822.

(6) Wilbuer, A.; Vlecken, D. H.; Schmitz, D. J.; Kräling, K.; Harms, K.; Bagowski, C. P.; Meggers, E. *Angew. Chem., Int. Ed.* **2010**, *49*, 3839–3842.

(7) For work from other groups on the design of metal-containing protein kinase inhibitors, see: (a) Spencer, J.; Mendham, A. P.; Kotha, A. K.; Richardson, S. C. W.; Hillard, E. A.; Jaouen, G.; Male, L.; Hursthouse, M. B. *Dalton Trans.* **2009**, 918–921. (b) Biersack, B.; Zoldakova, M.; Effenberger, K.; Schobert, R. *Eur. J. Med. Chem.* **2010**, *45*, 1972–1975.

(8) Feng, L.; Geisselbrecht, Y.; Blanck, S.; Wilbuer, A.; Atilla-Gokcumen, G. E.; Filippakopoulos, P.; Kräling, K.; Celik, M. A.; Harms, K.; Maksimoska,

J.; Marmorstein, R.; Frenking, G.; Knapp, S.; Essen, L.-O.; Meggers, E. *J. Am. Chem. Soc.* **2011**, *133*, 5976–5986.
(9) Meggers, E.; Atilla-Gokcumen, G. E.; Bregman, H.; Maksimoska, J.; Mulcahy, S. P.; Pagano, N.; Williams, D. S. *Synlett* **2007**, *8*, 1177–1189.
(10) (a) Bregman, H.; Williams, D. S.; Meggers, E. *Synthesis* **2005**, 1521–1527. (b) Pagano, N.; Maksimoska, J.; Bregman, H.; Williams, D. S.; Webster, R. D.; Xue, F.; Meggers, E. *Org. Biomol. Chem.* **2007**, *5*, 1218–1227.
(11) Manning, G.; Whyte, D. B.; Martinez, R.; Hunter, T.; Sudarsanam, S. *Science* **2002**, *298*, 1912–1934.
(12) Gill, T. P.; Mann, K. R. *Organometallics* **1982**, *1*, 485–488.
(13) This should be analogous to transition-metal−perfluoroalkyl complexes, which typically possess stronger M−C bonds compared to their nonfluorinated counterparts. See, for example: Elschenbroich, C. *Organometallics*, 3rd ed.; Wiley-VCH: Weinheim, Germany, 2006.
(14) Landgrafe, C.; Sheldrick, W. S. *Dalton Trans.* **1994**, 1885–1893.
(15) See, for example: (a) Ryabov, A. D.; Sukharev, V. S.; Alexandrova, L.; Le Lagadec, R.; Pfeffer, M. *Inorg. Chem.* **2001**, *40*, 6529–6532. (b) Bregman, H.; Carroll, P. J.; Meggers, E. *J. Am. Chem. Soc.* **2006**, *128*, 877–884. (c) Mulcahy, S. P.; Gründler, K.; Frias, C.; Wagner, L.; Prokop, A.; Meggers, E. *Dalton Trans.* **2010**, *39*, 8177–8182.
(16) For analogous reactions, see: (a) Fernandez, S.; Pfeffer, M.; Ritleng, V.; Sirlin, C. *Organometallics* **1999**, *18*, 2390–2394. (b) Leyva, L.; Sirlin, C.; Rubio, L.; Franco, C.; Le Lagadec, R.; Spencer, J.; Bischoff, P.; Gaiddon, C.; Loeffler, J.-P.; Pfeffer, M *Eur. J. Inorg. Chem.* **2007**, 3055–3066. (c) Djukic, J.-P.; Sortais, J.-B.; Barloy, L.; Pfeffer, M. *Eur. J. Inorg. Chem.* **2009**, 817–853.
(17) Fabian, M. A.; et al. *Nat. Biotechnol.* **2005**, *23*, 329–336.
(18) Karaman, M. W.; et al. *Nat. Biotechnol.* **2008**, *26*, 127–132.
(19) Katoh, K.; Kano, Y.; Ookawara, S. *Trends Cell Mol. Biol.* **2005**, *1*, 83–88.
(20) Cheng, Y.-C.; Prusoff, W. H. *Biochem. Pharmacol.* **1973**, *22*, 3099–3108.
(21) Uehata, M.; Ishizaki, T.; Satoh, H.; Ono, T.; Kawahara, T.; Morishita, T.; Tamakawa, H.; Yamagami, K.; Inui, J.; Maekawa, M.; Narumiya, S. *Nature* **1997**, *389*, 990–994.
(22) Bollag, G.; et al. *Nature* **2010**, *467*, 596–599.
(23) Flaherty, K. T.; Puzanov, I.; Kim, K. B.; Ribas, A.; McArthur, G. A.; Sosman, J. A.; O'Dwyer, P. J.; Lee, R. J.; Grippo, J.; Nolop, K.; Chapman, P. B. *New Engl. J. Med.* **2010**, *363*, 809–819.
(24) Berg, K.; Zhai, L.; Chen, M.; Kharazmi, A.; Owen, T. C. *Parasitol. Res.* **1994**, *80*, 235–239.
(25) Pinto-Bazurco Mendieta, M. A. E.; Negri, M.; Jagusch, C.; Hille, U. E.; Müller-Vieira, U.; Schmidt, D.; Hansen, K.; Hartmann, R. W. *Bioorg. Med. Chem. Lett.* **2008**, *18*, 267–273.
(26) Brotschi, C.; Mathis, G.; Leumann, C. J. *Chem. Eur. J.* **2005**, *11*, 1911–1923.
(27) Ranger, M.; Rondeau, D.; Leclerc, M. *Macromolecules* **1997**, *30*, 7686–7691.
(28) Kündig, E. P.; Monnier, F. R. *Adv. Synth. Catal.* **2004**, *346*, 901–904.
(29) Fang, D.; Nguyen, T. K.; Leishear, K.; Finko, R.; Kulp, A. N.; Hotz, S.; Van Belle, P. A.; Xu, X.; Elder, D. E.; Herlyn, M. *Cancer Res.* **2005**, *65*, 9328–9337.
(30) Hsu, M.-Y.; Shih, D.-T.; Meier, F. E.; Van Belle, P.; Hsu, J.-Y.; Elder, D. E.; Buck, C. A.; Herlyn, M. *Am. J. Pathol.* **1998**, *153*, 1435–1442.
(31) Fukunaga-Kalabis, M.; Martinez, G.; Liu, Z. J.; Kalabis, J.; Mrass, P.; Weninger, W.; Firth, S. M.; Planque, N.; Perbal, B.; Herlyn, M. *J. Cell Biol.* **2006**, *175*, 563–569.
(32) Spek, A. L. *PLATON, A Multipurpose Crystallographic Tool*; Utrecht University, Utrecht, The Netherlands, 1998.
(33) *X-AREA, Version 1.54*; STOE & Cie GmbH, 2009.
(34) Altomare, A.; Cascarano, G.; Giacovazzo, C.; Guagliardi, A. *J. Appl. Crystallogr.* **1993**, *26*, 343–350.
(35) Burla, M. C.; Caliandro, R.; Camalli, M.; Carrozzini, B.; Cascarano, G. L.; De Caro, L.; Giacovazzo, C.; Polidori, G.; Siliqi, D.; Spagna, R. *J. Appl. Crystallogr.* **2007**, *40*, 609–613.
(36) Sheldrick, G. M. *Acta Crystallogr., Sect. A* **2008**, *64*, 112–122.